

# Comparison of simulations and data from a seismo-acoustic tank experiment

Jon M. Collis<sup>a)</sup> and William L. Siegmann  
*Rensselaer Polytechnic Institute, Troy, New York 12180*

Michael D. Collins, Harry J. Simpson, and Raymond J. Soukup  
*Naval Research Laboratory, Washington, D.C. 20375*

(Received 7 February 2007; revised 16 June 2007; accepted 19 June 2007)

A tank experiment was carried out to investigate underwater sound propagation over an elastic bottom in flat and sloping configurations. The purpose of the experiment was to evaluate range-dependent propagation models with high-quality experimental data. The sea floor was modeled as an elastic medium by a polyvinyl chloride slab. The relatively high rigidity of the slab requires accounting for shear waves in this environment. Acoustic measurements were obtained along virtual arrays in the water column using a robotic apparatus. Elastic parabolic equation solutions are in excellent agreement with data. © 2007 Acoustical Society of America.

[DOI: 10.1121/1.2756968]

PACS number(s): 43.30.Zk, 43.30.Ma [RCG]

Pages: 1987–1993

## I. INTRODUCTION

The ocean bottom has a major effect on shallow water sound propagation. The sediment can often be modeled as a fluid, but shear effects are important in some cases. The interface between the ocean and sediment can be modeled as horizontal in some cases, but its slope must be taken into account in many applications. Previous calculations have combined bottom effects and sloping fluid-solid interfaces, using parabolic equation,<sup>1,2</sup> spectral,<sup>3–5</sup> and hybrid<sup>6,7</sup> approaches. However, the combination of shear effects and bottom slope is a difficult problem to model accurately and efficiently. The parabolic equation method is an effective approach for solving such range-dependent seismo-acoustics problems,<sup>8,9</sup> including anisotropic<sup>10</sup> and interface wave effects.<sup>11</sup> Recent progress has improved the accuracy of this approach for problems involving sloping interfaces.<sup>12,13</sup>

Due to the difficulty in collecting high-quality experimental data, there have been relatively few experiments conducted which were capable of verifying the predictions of underwater sound models. Recent experiments focused on propagation up a wedge,<sup>14</sup> three-dimensional effects,<sup>15</sup> and rough surface backscattering.<sup>16</sup> Although tank experiments of acoustic propagation have established the significance of elastic effects they did not involve detailed field comparisons.<sup>17–19</sup> As a result, no definitive reference exists which validates range-dependent elastic parabolic equation models against high-quality experimental data.

In this paper, we compare parabolic equation solutions with data from an experiment involving a slab of polyvinyl chloride (PVC) that was suspended in a tank of water. For this scaled model of both flat and sloping elastic ocean bottoms, high-quality data were obtained by using a robotic apparatus to move a hydrophone along virtual arrays. The elas-

tic parameters of the slab were measured prior to the experiment. We were unable to obtain acoustic/fluid parabolic equation solutions that agree even approximately with the data. When shear was included in the model, we were able to achieve excellent agreement by fine tuning the geometric parameters. The experiment is reviewed in Sec. II. A discussion of the computer scale model and inversion procedures is given in Sec. III. Comparisons with parabolic equation solutions are presented in Sec. IV.

## II. TANK EXPERIMENT

A series of laboratory experiments with scale models of an elastic ocean bottom are being performed in order to test predictions of seismo-acoustic models. Here we report on the first Elastic Parabolic Equation Experiment (EPE 1), which was carried out in April 2004 inside a large fresh water tank at the Naval Research Laboratory.<sup>20</sup> An elastic bottom was modeled using a PVC slab (122×122×10 cm) from San Diego Plastics. The slab was suspended in water by cables, which were attached to its corners to minimize reflections. Source and receiver hydrophones were positioned over the slab using a robotic apparatus that allowed for accurate positioning. The slab, cables, source and receiver alignments, and robotic arms are illustrated in Fig. 1. The source, closer to the edge of slab, was fixed while the receiver moved at 2 mm increments away from the source. (An experiment with similar instrumentation and a milled PVC slab was performed a month later and is documented in Ref. 21.)

During EPE-1 the water temperature was maintained so that the sound speed remained within 1 m/s of 1482 m/s. As discussed in Ref. 20, estimates for the elastic properties of the slab in the band 300 kHz–1.5 MHz were obtained by transmitting pulses through a sample of the material. Results at 300 kHz are summarized in Table I, with estimated relative errors shown in the second column. Since this frequency band is at the high end of the transmitted frequency band of

<sup>a)</sup>Present address: Boston University, Boston, Massachusetts. Electronic mail: jcollis@bu.edu

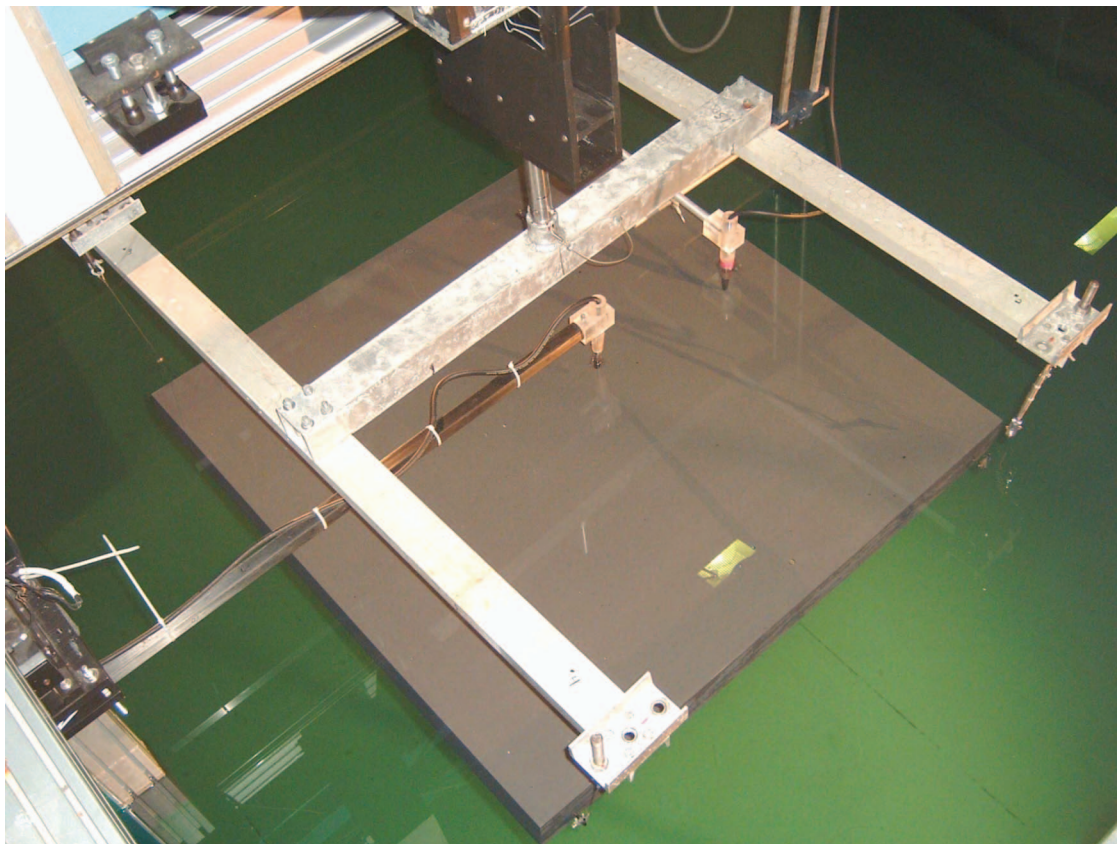


FIG. 1. The experimental setting; the PVC slab is suspended in water by cables attached near its corners. The robotic apparatus which positions the source and receiver hydrophones is shown.

the acoustic tank experiment, using the values at lower frequencies may introduce an extrapolation error.

The transmitted waveform was an impulse with a flat frequency spectrum over the band 100–300 kHz. A reference measurement was made by positioning the source and receiver 1 m apart and measuring the pressure produced from a shaped pulse which was flat within the source band. Figure 2 shows the temporal and frequency responses for the reference measurement. Measurements were recorded at 8192 points with a  $0.5 \mu\text{s}$  sampling interval. Windowing was applied to eliminate reflections from the hardware and the walls of the tank. The windowed time series were Fourier transformed, resulting in 4096 data points which spanned 1 MHz in the frequency domain. A transfer function was obtained by multiplying the frequency response with the reciprocal of the spectrum of the reference pulse.

Experimental runs were conducted in two environments with different source and receiver configurations. To show

TABLE I. Estimated physical values, with associated error estimates, of elastic PVC properties at 300 kHz (see Ref. 20).

Parameter	Value	Relative Error ( $\pm\%$ )	Absolute Error
Density ( $\text{kg}/\text{m}^3$ )	1378	0.5	7
Compressional speed (m/s)	2290	0.5	10
Compressional attenuation (dB/m)	0.33	2	0.01
Shear speed (m/s)	1050	0.5	5
Shear attenuation (dB/m)	1.00	4	0.04

the analogy between propagation in the tank and an ocean waveguide, we present acoustic propagation calculations at a scale of 1000:1 in Fig. 3, where the frequencies and lengths have been appropriately modified. The (constant) compressional and shear attenuation  $\alpha_p$  and  $\alpha_s$  in the units  $\text{dB}/\lambda$  ( $\lambda$  being the acoustic wavelength) are invariant under the scaling, because they are implicitly scaled with the wavelength. The first environment is essentially range independent (nearly horizontal slab), and a sample of calculated transmission loss contours is shown in Fig. 3(a) for a 100 Hz source. Also shown are the geometrical parameters: source depth  $z_s$  (which can be near the middle of the water column or near the bottom), depth of the slab below the source  $z_0$ , and depth of the opposite edge of the slab  $z_1$ . The receiver depth  $z_r$ , is not shown. Nominal values of these parameters are given in the second column of Table II. For the first two runs, the slab was suspended nearly parallel to the air-water interface. The propagation track was centered on the slab, with the source 15 cm away from the edge. The receiver was moved horizontally between 25 and 135 cm from the edge of the slab nearest the source to produce a virtual horizontal array with a spacing of 2 mm. The slab attenuated acoustic energy sufficiently to prevent spurious reflections from the slab bottom. For the last two runs, the environment is range dependent, with the slab sloping as illustrated in Fig. 3(b). Nominal values of the geometrical parameters shown in Fig. 3(b) are given in the second column of Table III. In the time period between the positioning of the source and receiver in the tank and the data collection, it is estimated that the depth of

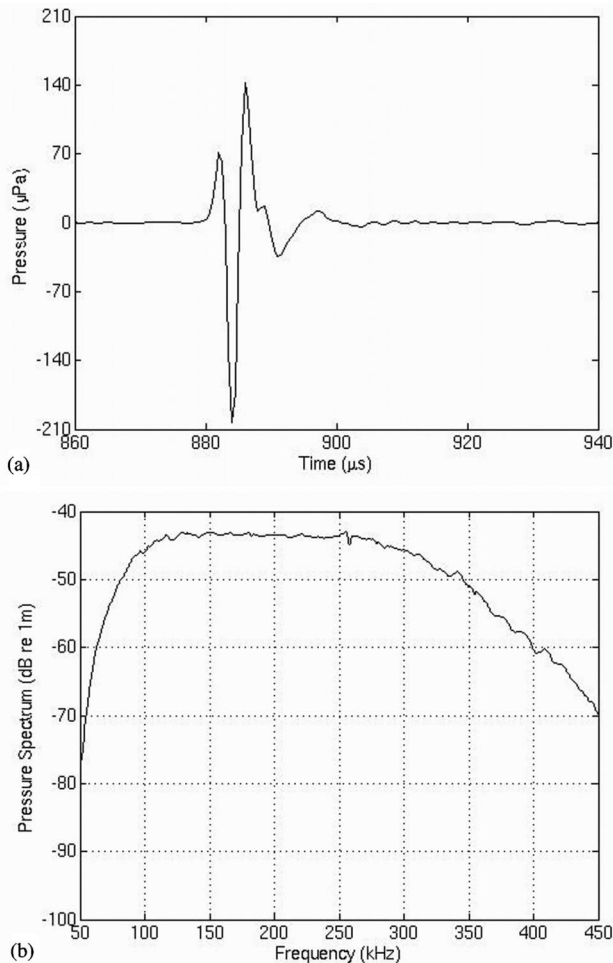


FIG. 2. Reference measurements of the source and receiver separated by 1 m. (a) Temporal response plot of pressure ( $\mu\text{Pa}$ ) vs time ( $\mu\text{s}$ ). (b) The frequency response plotted as power spectral density vs frequency (kHz). The frequency response was designed to be flat in the 100–300 kHz band.

the slab, source and receiver could have decreased by as much as 6 mm due to evaporation of water from the tank. This evaporation affected the geometrical parameters in an analogous manner for both the flat and sloped slab cases, as the source and receiver were re-positioned prior to the sloped slab data acquisition. Additional uncertainty in the geometrical parameters could arise from a non-central acoustic source location inside the spherical object (of radius 1 cm) and slight deviations from flatness for the slab.

### III. PROPAGATION CALCULATIONS

Experimental data were compared with calculations from a parabolic equation model suitable for range-dependent environments and fluid or elastic media. Because parabolic equation solutions are exact in range-independent environments and highly accurate in range-dependent environments, we anticipate close comparisons with data, provided accurate estimates of geometric and material parameter values are available. Initial comparisons of data and calculations using the measured and recorded parameter values suggested the need for refinement. Two inversion procedures, using an elastic parabolic equation model, were used to determine precise estimates. First, forward iterations at selected

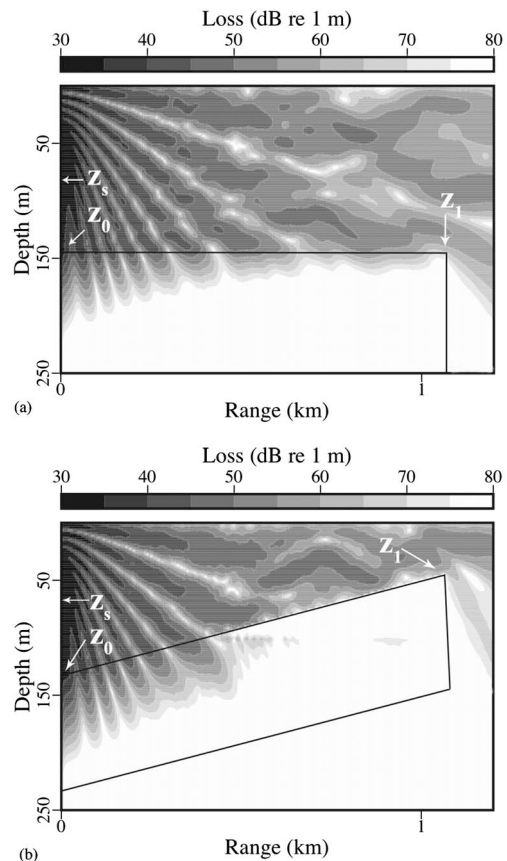


FIG. 3. Calculated transmission loss contours for the compressional field of a 100 Hz mid-depth source using scaled parameters for length and frequency: (a) flat case, (b) sloped case.

frequencies were performed, and parameter values were found that minimized the vector norm of transmission loss differences. Second, simulated annealing inversions<sup>22–24</sup> were run at those frequencies to refine the values. Deep fades (local minima) in transmission loss patterns were sufficiently rare and narrow enough to not affect the inversion results. The simulated annealing algorithm is based on the coordinate rotation approach of Ref. 22. We selected parameter values by averaging results over the five nominal frequencies 100, 150, 200, 250, and 300 kHz.

Results from the two inversion processes are given in Tables II and III for the flat and sloped cases. When comparing values obtained from the inversions with the nominally recorded values, the differences are generally less than 10%. The maximum difference of 22% occurs with the shallow receiver in the sloped case, although the absolute error for this case is small. The largest absolute error (12 mm) occurs for the deep source in the sloping configuration and probably results from a combination of uncertainties due to evaporation and in slab/source depths. The actual differences for all other values, of 1 cm or less, reflect the precision required for accurate comparisons. For example, the flat case is nominally horizontal within 1 mm, but this deviation is sufficient to distort the comparisons observably. The refinements in values obtained by using simulated annealing after forward iterations are small, but they result in improvements in all cases.

TABLE II. Inversion results for geometric parameters: for the flat slab case. Nominal values are according to the experimental plan; other values are from two inversion procedures. Estimates from simulated annealing yield better agreement with data. Errors are between nominal and simulated annealing results.

Flat case	Nominal	Iterative	Simulated annealing	Absolute error	Relative error ( $\pm\%$ )
$z_s$ mid (cm)	7.50	6.91	6.91	0.59	7.9
$z_s$ deep (cm)	14.55	13.63	13.68	0.87	6.0
$z_r$ (cm)	14.55	13.74	13.71	0.84	5.8
$z_0$ (cm)	15.00	14.44	14.47	0.53	3.6
$z_1$ (cm)	15.00	14.55	14.54	0.46	3.1

#### IV. COMPARISONS OF MEASUREMENTS AND CALCULATIONS

Data comparisons were made with parabolic equation implementations for fluid<sup>25</sup> and elastic media. The elastic model uses a variable rotated elastic parabolic equation.<sup>13</sup> Results are presented for selected geometries and source frequencies of 125,200, and 275 Hz. For all calculations, the water sound speed is 1482 m/s and the slab density, sound speeds, and attenuations are the measured values from Table I. Computations were made to the effective maximum range of 120 cm.

##### Range-independent propagation

We first consider examples of the nominally flat case, which actually has weak range dependence. The source is located at either mid-depth ( $z_s=6.91$  cm) or deep ( $z_s=13.68$  cm). The values of  $z_r$ ,  $z_0$ , and  $z_1$  are given in the fourth column of Table II, where the depth  $z_1$  is measured at  $r=106.8$  cm. Figure 4 shows comparisons between the elastic solution and data for the mid-depth source. There is excellent agreement between these calculations and the data, with only subtle differences observed in the patterns. The elastic parabolic equation solution closely tracks detailed variations in the transmission loss. Deep source results are illustrated in Figs. 5 and 6 for both fluid and elastic parabolic equation calculations. Solutions in Fig. 5 for the fluid parabolic equation show significant differences from data and only manage to capture the basic trend of the data curves. Close to the source, the fluid solutions track the interference pattern and agree fairly well with measurements, but they seriously underestimate the loss as range increases. In contrast, solutions from the elastic parabolic equation are plotted in Fig. 6. For all three frequencies these solutions provide close matches to both the interference pattern and amplitude

of the measured transmission loss. Although the fields differ dramatically for the two source positions, both are accurately modeled by the elastic parabolic equation solutions. The field structure is somewhat more complicated with the deep source position, but the solutions still handle the precise phase and amplitude changes of the pattern well. Beyond the edge of the slab, the field differs slightly from the data.

##### Range-dependent propagation

Figure 7 shows elastic model calculations and data for range-dependent propagation over an approximately  $4.8^\circ$  slope, for the case where the source is at mid-depth and the receiver is near-surface. The values of  $z_s$ ,  $z_r$ ,  $z_0$ , and  $z_1$  used in the calculations are in the fourth column of Table III, where the depth at  $z_1$  is measured at  $r=106.5$  cm. There is excellent agreement between the calculated and recorded values, with fine details of the field resolved to high accuracy. An extensive collection of additional sloping bottom cases for other frequencies and source and receiver positions was investigated, and the fields in all cases are very well represented by the elastic parabolic equation calculations.

#### V. CONCLUSIONS

Our main conclusion is the demonstration of excellent agreement between elastic parabolic equation solutions and experimentally recorded values for sound propagation in water overlying an elastic slab. The agreement confirms that the elastic parabolic equation is capable of resolving both nearly range-independent and range-dependent problems efficiently and precisely. The results obtained for the range-dependent sloped case provide support for the validity of the parabolic equation derivation in its elastic formulation. The fine details of the transmission loss pattern that are resolved by the elastic solutions represent benchmark accuracy agreement with

TABLE III. Inversion results for geometric parameters: sloped case. Nominal values are according to the experimental plan; other values are from two inversion procedures. Estimates from simulated annealing yield better agreement with data. Errors are between nominal and simulated annealing results.

Sloped case	Nominal	Iterative	Simulated annealing	Absolute error	Relative error ( $\pm\%$ )
$z_s$ mid (cm)	6.90	6.34	6.34	0.56	8.2
$z_s$ deep (cm)	13.55	12.43	12.35	1.2	8.9
$z_r$ (cm)	2.00	1.57	1.56	0.44	22
$z_0$ (cm)	13.80	13.34	13.29	0.51	3.7
$z_1$ (cm)	4.95	4.55	4.54	0.41	8.2

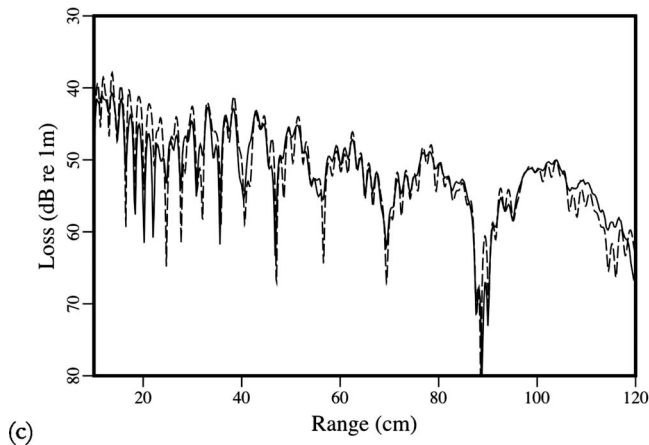
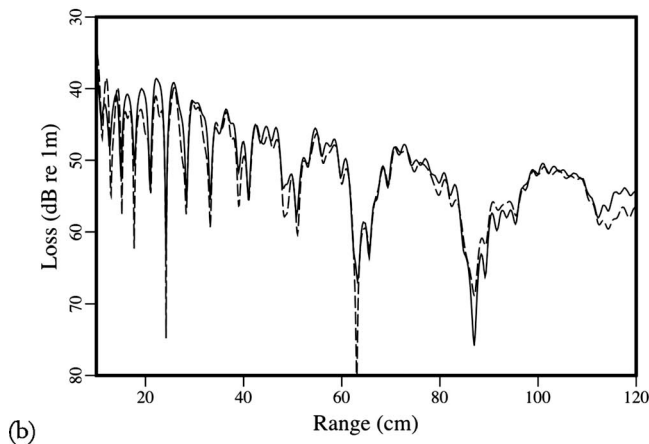
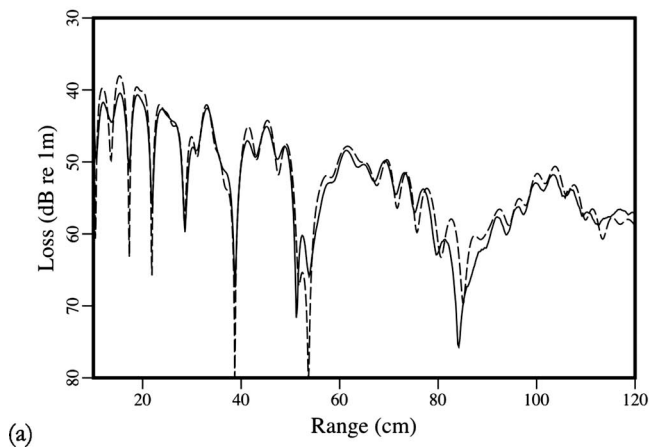


FIG. 4. Transmission loss vs range for the flat case, mid-depth source at 6.91 cm and near-bottom receiver at 13.71 cm. Comparisons show data (solid curve) and calculations from the elastic parabolic equation (dashed curve), for source frequencies: (a) 125 kHz, (b) 200 kHz, and (c) 275 kHz.

the data. Another conclusion is the demonstration of the expected poor agreement between fluid parabolic equation solutions and recorded values. In combination with the excellent agreement of the elastic solution, this result shows that the fluid parabolic equation is unsatisfactory for modeling underwater sound propagation over bottoms with significant elasticity.

Iteration by inversion methods for values of the geometric parameters was essential as the evaporation of water from the tank and other uncertainties in the source and receiver

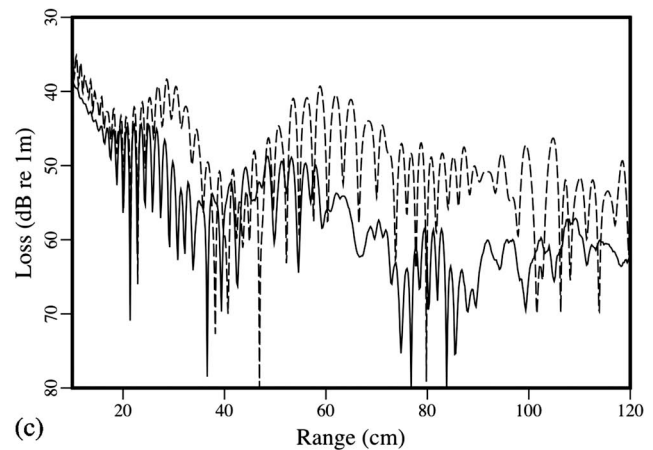
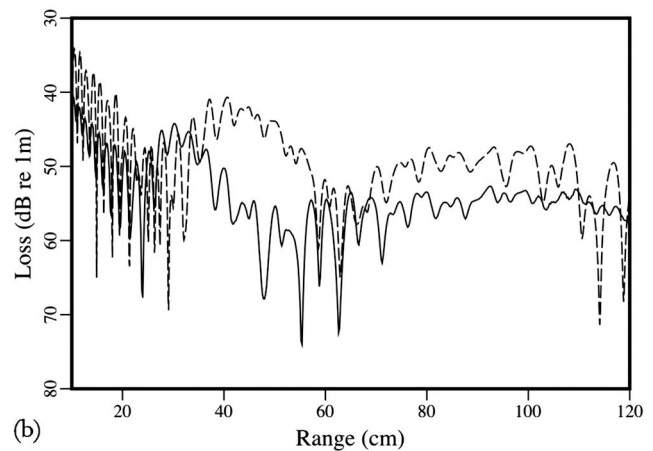
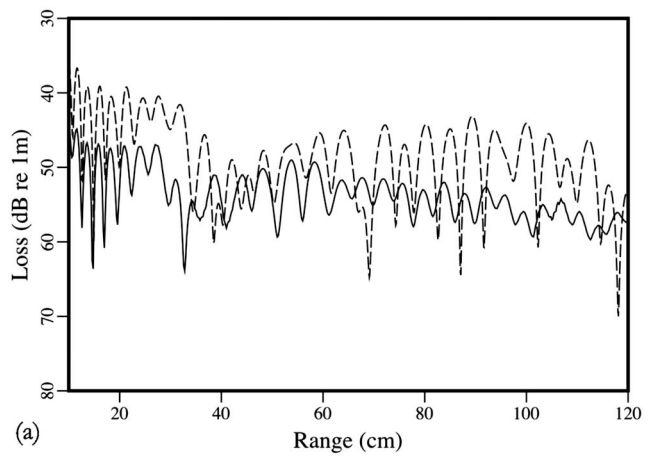


FIG. 5. Transmission loss vs range for the flat case, deep source at 13.69 cm, and near-bottom receiver at 13.71 cm. Comparisons show data (solid curve) and calculations from the fluid parabolic equation RAM (dashed curve), for source frequencies: (a) 125 kHz, (b) 200 kHz, and (c) 275 kHz.

position and the slab surface hat to be taken into account. The success of the elastic PE model in obtaining excellent agreement with data, given these adjustments, illustrates the sensitivity of acoustic propagation in a simple waveguide to small changes in the experimental geometry. The detailed agreement illustrates that the elastic PE code could be used to successfully model a simulated waveguide for which the

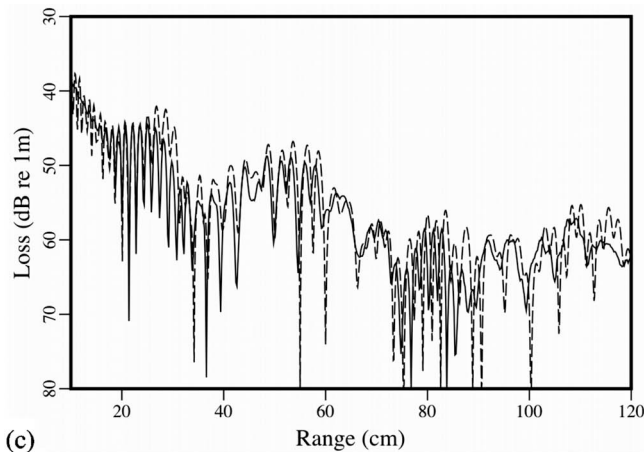
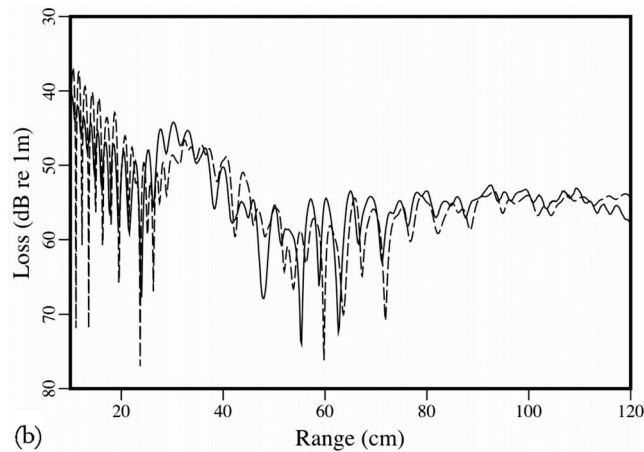
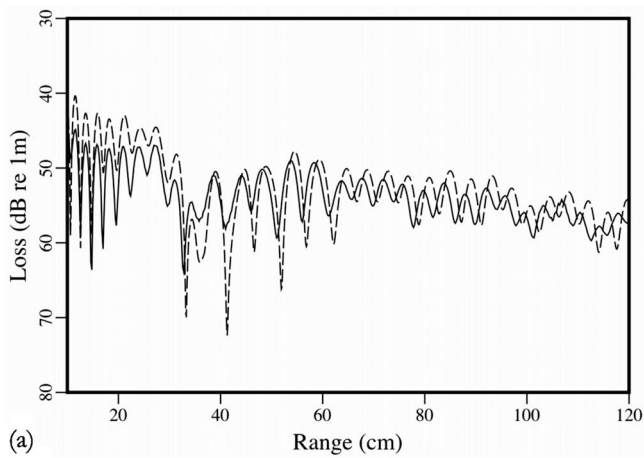


FIG. 6. Transmission loss vs range for the flat case, deep source at 13.69 cm and near-bottom receiver at 13.71 cm. Comparisons show data (solid curve) and calculations from the elastic parabolic equation (dashed curve), for source frequencies: (a) 125 kHz, (b) 200 kHz, and (c) 275 kHz.

where properties of the bottom are of great importance. Future work will focus on more complex varieties of range dependence.

#### ACKNOWLEDGMENTS

We thank Dr. De-Hua Han at the University of Houston Rock Physics Laboratory for his measurements of geoacoustic values of the elastic slab included in Ref. 20. This work

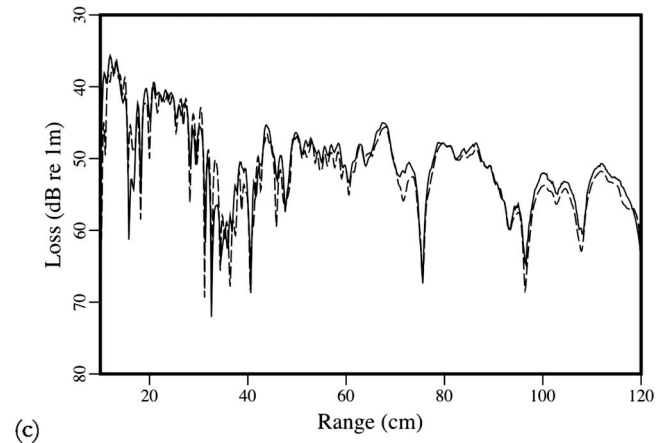
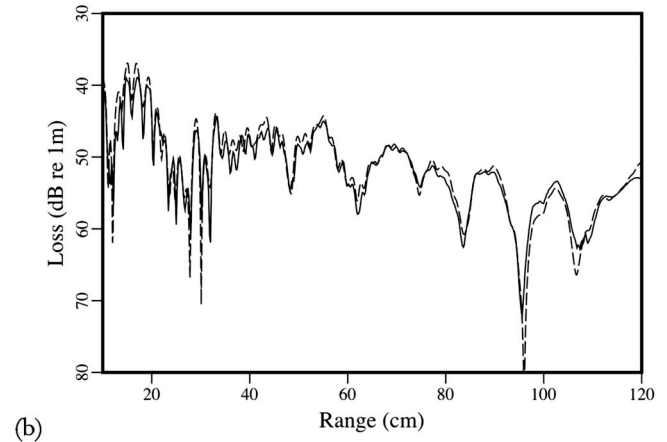
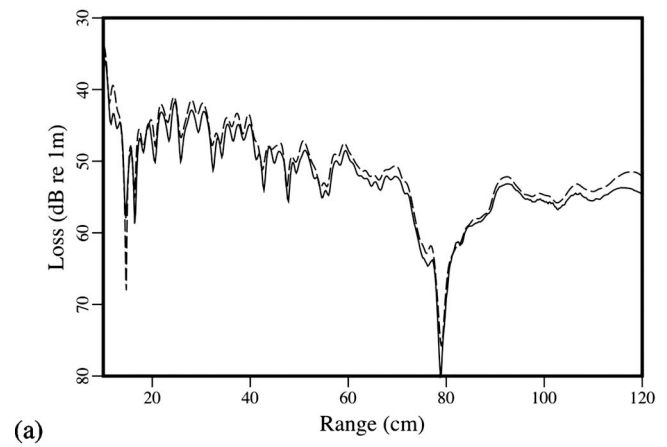


FIG. 7. Transmission loss vs range for the sloped case, mid-depth source at 6.34 cm and near-surface receiver at 1.56 cm. Comparisons show data (solid curve) and calculations from the elastic parabolic equation (dashed curve), for source frequencies: (a) 125 kHz, (b) 200 kHz, and (c) 275 kHz.

was supported by the Office of Naval Research, including an ONR Ocean Acoustics Graduate Traineeship Grant to the first author.

<sup>1</sup>M. D. Collins, "A higher-order parabolic equation for wave propagation in an ocean overlying an elastic bottom," *J. Acoust. Soc. Am.* **86**, 1459–1464 (1989).

<sup>2</sup>M. D. Collins, "The rotated parabolic equation and sloping ocean bottoms," *J. Acoust. Soc. Am.* **87**, 1035–1037 (1990).

<sup>3</sup>J. T. Goh, H. Schmidt, P. Gerstoft, and W. Seong, "Benchmarks for validating range-dependent seismo-acoustic propagation codes," *IEEE J. Ocean. Eng.* **22**, 226–236 (1997).

- <sup>4</sup>I. T. Lu and L. B. Felsen, "Adiabatic transforms for spectral analysis and synthesis of weakly range-dependent shallow ocean Green's functions," *J. Acoust. Soc. Am.* **81**, 897–911 (1987).
- <sup>5</sup>J. T. Goh and H. Schmidt, "Validity of spectral theories for weakly range-dependent ocean environments—numerical results," *J. Acoust. Soc. Am.* **95**, 727–732 (1994).
- <sup>6</sup>H. Schmidt, W. Seong, and J. T. Goh, "Spectral super-element approach to range-dependent ocean acoustic modeling," *J. Acoust. Soc. Am.* **98**, 465–472 (1995).
- <sup>7</sup>J. T. Goh and H. Schmidt, "A hybrid coupled wavenumber integration approach to range-dependent ocean acoustic modeling," *J. Acoust. Soc. Am.* **100**, 1409–1420 (1996).
- <sup>8</sup>F. B. Jensen, W. A. Kuperman, M. B. Porter, and H. Schmidt, *Computational Ocean Acoustics* (Springer-Verlag, New York, 2000), pp. 325–389.
- <sup>9</sup>M. D. Collins, "Higher-order parabolic approximations for accurate and stable elastic parabolic equations with application to interface wave propagation," *J. Acoust. Soc. Am.* **89**, 1050–1057 (1991).
- <sup>10</sup>A. J. Fredricks, W. L. Siegmann, and M. D. Collins, "A parabolic equation for anisotropic elastic media," *Wave Motion* **31**, 139–146 (2000).
- <sup>11</sup>W. Jerzak, W. L. Siegmann, and M. D. Collins, "Modeling Rayleigh and Stoneley waves and other interface and boundary effects with the parabolic equation," *J. Acoust. Soc. Am.* **117**, 3497–3503 (2005).
- <sup>12</sup>M. D. Collins and D. K. Dacol, "A mapping approach for handling sloping interfaces," *J. Acoust. Soc. Am.* **107**, 1937–1942 (2000).
- <sup>13</sup>D. A. Outing, W. L. Siegmann, M. D. Collins, and E. K. Westwood, "Generalization of the rotated parabolic equation to variable slopes," *J. Acoust. Soc. Am.* **120**, 3534–3538 (2006).
- <sup>14</sup>S. A. L. Glegg, G. B. Deane, and I. G., House, "Comparison between theory and model scale measurements of three-dimensional sound propagation in a shear supporting penetrable wedge," *J. Acoust. Soc. Am.* **94**, 2334–2342 (1993).
- <sup>15</sup>J. P. Sessarego, "Scaled models for underwater acoustics and geotechnics applications," *Proceedings of the Sixth European Conference on Underwater Acoustics*, Gdansk, Poland (2002).
- <sup>16</sup>R. J. Soukup, G. Canepa, H. J. Simpson, J. E. Summers, and R. F. Gragg, "Small-slope simulation of acoustic backscatter from a physical model, *J. Acoust. Soc. Am.*, in press.
- <sup>17</sup>I. Tolstoy, "Shallow water test of the theory of layered wave guides," *J. Acoust. Soc. Am.* **30**, 348–361 (1958).
- <sup>18</sup>I. Tolstoy, "Guided waves in a fluid with continuously variable velocity overlying an elastic solid: Theory and experiment," *J. Acoust. Soc. Am.* **32**, 81–87 (1960).
- <sup>19</sup>R. K. Eby, A. O. Williams, R. P. Ryan, and P. Tamarkin, "Study of acoustic propagation in a two-layered model," *J. Acoust. Soc. Am.* **32**, 88–99 (1960).
- <sup>20</sup>R. J. Soukup, H. J. Simpson, E. C. Porse, J. E. Summers, and R. F. Gragg, "Geoacoustic physical modeling elastic parabolic equation 1 (GPM EPE1) experiment: Measurement report and acoustic data," U.S. Naval Research Laboratory Memo. Rep. 7140-04-8826 (2004).
- <sup>21</sup>R. J. Soukup, H. J., Simpson, E. C. Porse, J. E. Summers, and R. F. Gragg, "Geoacoustic physical modeling rough surface scattering experiment 2 (GPM RSS2): Measurement report, acoustic data and profilometry," U.S. Naval Research Laboratory Memo. Rep. 7140-04-8827 (2004).
- <sup>22</sup>M. D. Collins and L. Fishman, "Efficient navigation of parameter landscapes," *J. Acoust. Soc. Am.* **98**, 1637–1644 (1995).
- <sup>23</sup>M. D. Collins, W. A. Kuperman, and H. Schmidt, "Nonlinear inversion for ocean-bottom properties," *J. Acoust. Soc. Am.* **92**, 2770–2783 (1992).
- <sup>24</sup>R. J. Cederberg and M. D. Collins, "Applications of an improved self-starter to geoacoustic inversion," *IEEE J. Ocean. Eng.* **22**, 102–109 (1997).
- <sup>25</sup>M. D. Collins, "User's Guide for RAM Versions 1.0 and 1.0p", [ftp://ftp.ccs.nrl.navy.mil/pub/ram/RAM\(2006\)](ftp://ftp.ccs.nrl.navy.mil/pub/ram/RAM(2006)).